Procedure for Selection of Switchgear Parameters for Safe Operation of Electric Distribution Network

T.O. Akinbulire, P.O. Oluseyi* and F.O. Eruotor
Department of Electrical and Electronics Engineering, University of Lagos, Lagos, Nigeria
*Corresponding author email: poluseyi@unilag.edu.ng

ABSTRACT
One of the major hazards of short circuit is "Arc Flash" incidence which is established when current flows through ionized air that eventually leads to expelled molten metal in the form of arcs. This results in very high ambient temperature around the switchgear connecting system. The best approach to mitigate the lethal and hazardous action of this thermal outbreak is by adopting appropriate sizing of the switchgear to withstand the expected 3-phase current-induced temperature excursion; so as to avoid the attendant system fault occurrence. In an attempt to determine the choice of the switchgear selection for this task, the power network protection analysis is modeled by the conventional techniques using the electrical load flow and short circuit analysis. The ensuing model is then treated to transient fault analysis protocols using various fault current values for the selection of appropriate size of the overcurrent protective devices (OCPD). This is thus simulated using Electrical Transient Analyzer Program (ETAP). From this development, a series of numerical results is obtained, in respect of the system short circuit capacity, under various operating conditions. When these results are compared with the industrial standard practices for effective operation of the distribution network, it is discovered that the switchgear equipment operates safely at a region within which its electrical current capacity is calibrated with much higher magnitude than the system's short circuit capacity. Hence for resilience against the arc flash induced network failure, it can then be concluded that the network should be subjected to a well calibrated and high precision electrically resilient, but thermally stable, current-based switchgear selection.

Keywords: Faults, Arc flash, Electric equipment, Switchgear, Hazard.

1.0 INTRODUCTION

In high and medium voltage (electrical) network; there is need for switchgears that could provide necessary protection and control action against fault occurrence. One of the major challenges is the appropriate sizing and choice of switchgear that would be able to handle such huge excursion of thermal and current magnitudes. In line with this, a principal factor in the selection of the ratings of switchgear (i.e. circuit breakers, fuses, relays, switchboards, etc.) is the magnitude of the anticipatory three-phase short circuit current (Yu et al. 1982). This then means that the protection gear should have appropriate trip setting as well as proper rating for it to withstand and isolate the high fault currents. To guarantee this, a shrewd and intelligent approach is essential for the appreciation and detection of the potential faults. In addition, the influence of this on the bus bars and switchboards cannot be overemphasized from the perspective of the intense mechanical forces associated with short circuits.

According to available records, the lifespan of a typical power infrastructure is within the range of 20 and 40 years (Davidson, 2005). However, this can be enhanced by excellent and well-structured regime of maintenance culture. Recently, with the introduction of asset management, utilities have moved from a time-based maintenance regime to a condition-based mode. This enables power utilities to extend service intervals. In which case, the condition assessment of facilities is carried out to determine the expected lifespan. This thus provides opportunity to make decision on whether there is need for the extension of the useful life of the equipment or outright replacement of it. In most cases, the latter is always encountered mid-way into the life of an equipment which may primarily be due to prolonged electrical overloading of such equipment. However, for every electrical network, it is very necessary to provide a very formidable protection against overcurrent events.

Hence, it is important to estimate the prospective current magnitude due to short circuit conditions and make adequate provision to withstand or interrupt such current. Thus, there is grave need to design the electrical protection scheme that would be able to withstand the advent of the resulting fault or arc flash occurrence in the network. This is achieved by modeling the essential protection components with respect to reliability, dependability, and security. In addition, the reinforcement of the network is essentially built to ensure that the restoration of service suffer minimal time lag. This is to ensure that the electrical network operates without noticeable power service disruption.

In most cases, the insulation failure because of fault occurrence often results in unconstrained excessive flow of current which leads to huge generation of heat. In other words, this could result in mechanical forces (stresses) which may result in tremendous damage to the power equipment (Warvick, 1997). Inadvertently, a short-circuit current generates heat which is proportional to the square of its current magnitude. This large amount of heat generated by the short circuit current has capacity to rupture the insulation of rotating machinery and other power apparatus which may be connected to the system. As a matter of fact, the immediate danger involved in this generated heat is that it tends to impair insulating materials to the point of permanent destruction. This also exerts harmful effects upon the contact parts of protective devices. However, this situation must not be allowed in protective devices if interrupting difficulties must be avoided.

A fault in the insulation of a circuit, in many cases, causes an arc at the point of the fault. Such an arc may be destructive and may result in fire hazard. Prolonged duration of arcing, in addition to the heat released, may result in transient over voltage phenomenon which may threaten the integrity of the insulation of equipment in other parts of the system (PSEC-IEEE, 2000). Clearly, the protective devices must be appropriately rated to ensure timely isolation of the fault section from the rest of the power system. To achieve this, Sarwa *et al.* (2019) articulated the scheme for the detection and isolation of high impedance fault (HIF) in a power distribution network. Their designed scheme utilized available data from voltage and current sensors whereby the technique deployed multiple algorithms for detecting and identifying high impedance fault. The results for different fault scenarios showed that the method created protocol which is fast and accurate in diagnosing high impedance faults (HIF). But the major drawback of the high impedance fault (HIF) detection techniques is that they are not capable of detecting all types of high impedance faults. Furthermore, active methods of HIF detection use signal injection which deteriorates the system's power quality. This setback is addressed in the work of Sarwar *et al*. (2019) by considering all faults and fault contributions thereby recording the highest possible short circuit magnitude before experiencing any system failure. Similarly, Chen *et al.* (2012) designed a nonlinear frequency analyzer to locate water tree degradation in power cables to resolve the problems associated with current off-line inspection-based diagnostic approaches. This technique essentially determines the location of water tree degradation without switching off power supply so as to significantly enhance the capability of power cable damage diagnosis. Numerical simulation results have demonstrated the effectiveness of the new technique and shown its potential to resolve the power cable damage location problem. The disadvantage of this method is that it can worsen the effect of data noise and may lead to unreliable detection results because it is meant to detect outliers in clusters with uniform density. From another perspective, an adaptive fault location algorithm was designed by Al-Mohammed and Abido (2014) for power system networks depending on synchronized phasor measurements using phasor measurement units (PMUs). The algorithm is

independent of any data from electric utility for better accuracy. This process suffers a setback for not considering the data from electric utility. Hence there is the need for a holistic approach as demonstrated by the work to evaluate the entire system component that could influence the network security. In another version developed by Wu *et al*. (2014), the methodology adopted is based on support vector machine (SVM). The technique is used for mapping a predetermined number of faults with fault detection, diagnosis, and online controller selection type reconfiguration mechanism. The methods in Wu *et al.* (2014) have a few shortcomings in respect of how to distinguish all the faults quickly and accurately in the Tennessee Eastern (TE) process by the SVM. It is noteworthy that if the selected number of features is not appropriate, useful information will be reduced. This leads to decrease in the dimension that may result in notable disadvantage in the fault diagnosis. Nevertheless, a MATLAB simulation-based fault detection was designed for an interconnected system by Preethi and Manik (2016). With the help of time synchronized phasor measurements and discrete Fourier transforms method, it compares positive sequence voltage magnitudes and positive sequence current phase difference angles for each interconnected line. This method generally has problems of distinguishing between traveling waves reflected from the fault point and from power system terminals, which decreases the reliability of the fault location method. In the same vein, Rambabu *et al*. (2015) presented a zone protection scheme using distance relay. In this scheme, single line to ground fault was created and impedance-based distance protection analysis was carried out. One of the main disadvantages of distance relays is the limited fault resistance measurement capability. The paper is based on transmission line, but the current investigation basically considers a typical power distribution network.

In other words, this current research investigates the appropriate rating of the distribution network's switchgear equipment to ensure satisfactory protection strategy that would adequately withstand fault current that could result in equipment damage. To this end, this is achieved by developing a model for the evaluation of current magnitude in the distribution system. Further to which a design protocol is established to reduce the possibility of stress on the switchgear components as well as the overall restoration time of the faulty system to service.

2.0 DESIGN METHODOLOGY

This current study utilized Electrical Transient Analysis Program (ETAP) software for the short circuit calculations. This is traditionally developed with its foundation squarely laid on the Newton-Raphson power flow technique. In which case, there are several methods of solving the resulting nonlinear system of equations. However, the adopted solution methodology begins with initial estimates of all unknown variables (i.e., voltage magnitude and angles at load buses and voltage angles at generator buses). Further to this, the Taylor Series is adopted, with the second and higher order terms ignored, for each of the power balance equations included in the system of equations. The result is a linear system of equation that can be expressed as depicted in equation (1):

$$\begin{bmatrix} \Delta\theta \\ \Delta|V| \end{bmatrix} = -J^{-1} \begin{bmatrix} \Delta P \\ \Delta Q \end{bmatrix} \quad (1)$$

In equation (1); ΔP and ΔQ are referred to as the mismatched equations between the scheduled and calculated values of real and reactive power quantities, respectively. While $\Delta\theta$ and $\Delta|V|$ are initial estimates of the voltage phase angle and voltage magnitude.

This is thus expressed in equation (2) as:

$$\Delta P_i = -P_i + \sum_{k=1}^{N} |V_i||V_k|(G_{ik}cos\theta_{ik} + B_{ik}sin_{ik}) \quad (2)$$
$$\Delta Q_i = -Q_i + \sum_{k=1}^{N} |V_i||V_k|(G_{ik}sin\theta_{ik} - B_{ik}cos_{ik})$$

For the calculated values, J^c is a matrix of partial derivatives known as the calculated Jacobian matrix which is expressed in equation (3) as follows:

$$J^c = \begin{bmatrix} \frac{\partial \Delta P^c}{\partial \theta^c} & \frac{\partial \Delta P^c}{\partial |V^c|} \\ \frac{\partial \Delta Q^c}{\partial \theta^c} & \frac{\partial \Delta Q^c}{\partial |V|^c} \end{bmatrix} \quad (3)$$

where P^c: calculated real power; Q^c: calculated reactive power.

V^c: calculated voltage magnitude; θ^c: calculated voltage phase angle

From equation 4; the calculated voltage components are obtained as shown in equation (4):

$$\begin{bmatrix} \Delta\theta^c \\ \Delta V^c \end{bmatrix} = \begin{bmatrix} \frac{\partial \Delta P^c}{\partial \theta^c} & \frac{\partial \Delta P^c}{\partial |V^c|} \\ \frac{\partial \Delta Q^c}{\partial \theta^c} & \frac{\partial \Delta Q^c}{\partial |V|^c} \end{bmatrix}^{-1} \begin{bmatrix} P_{sched} - P^c \\ Q_{sched} - Q^c \end{bmatrix} \quad (4)$$

Where P_{sched} and Q_{sched} are the scheduled real and reactive powers injected into the system respectively. As stated earlier; $\Delta\theta$ and $\Delta|V|$ are initial estimates of the voltage phase angle and voltage magnitude.

The linearized system of equations is solved to determine the updated estimate (i.e., m+1) of voltage magnitude and voltage phase angle based on equations (5) and (6):

$$\theta^{m+1} = \theta^m + \Delta\theta \quad (5)$$
$$|V|^{m+1} = |V|^m + \Delta|V| \quad (6)$$

The process continues until the stipulated stopping condition is attained.

2.1 Algorithm for the evaluation of short circuit current

There are some critical components of the power network that must be subjected to fault analysis to determine their respective resilience to system fault occurrence. These power utility components include the power generator, transformer, and such other power equipment. Thus, the procedure adopted for the manual calculation of 3-phase short circuit current is as depicted in Figure 1.

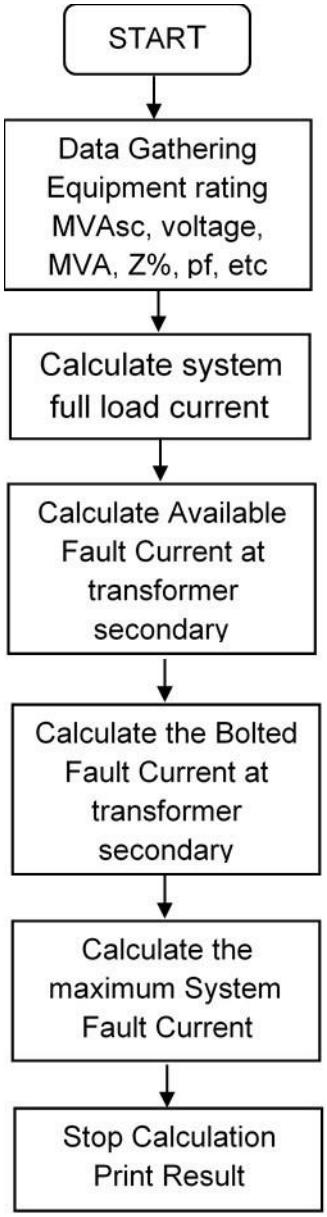


Figure 1. Flow chart for manual calculation of 3-phase short circuit fault

2.1.1 Transformer Fault Current

The calculation of the short circuit current when there is a transformer in the circuit is represented as shown in Figure 2. The analysis of this circuit is processed using equations (7) and (8).

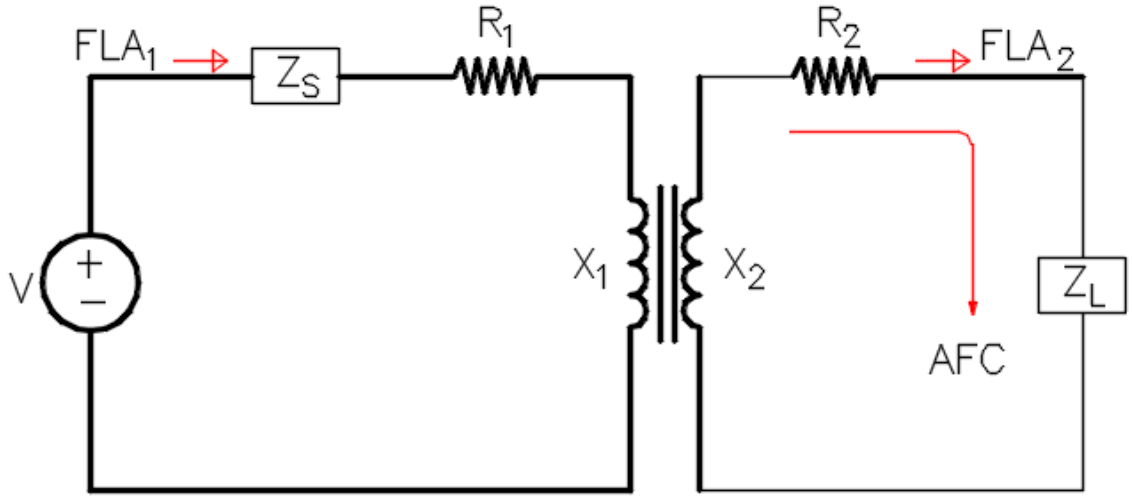


Figure 2. A simplified circuit diagram of transformer with short circuit.

During the assessment, the transformer is usually tagged with the "%tage" impedance value written on its nameplate. This is usually the laboratory-tested value as provided by the manufacturers. Hence, considering a 2000kVA, 11kV/415V transformer whose circuit diagram shown above is as follows.

Step 1: Determine the transformer full load amps (F.L.A.) of the system as generally expressed in equation (7).

$$\text{FLC(secondary)} = \frac{kVA_{3-phase}}{kV_{(L-L)}\sqrt{3}} \qquad (7)$$

Step 2: Calculate the available fault current (AFC) at the transformer secondary side simply gives equation (8).

$$\text{AFC(secondary)} = \frac{\text{FLA(secondary)} * 100}{\%Z} \text{ or } \frac{\text{FLA(secondary)}}{\%Z_{pu}} \qquad (8)$$

Note that the numerator of equation (8) has a multiple of 100 which when divided with %Z will result in $\%Z_{pu}$.

FLC = 2000 / 1.732 x 0.415 = 2,782.5A
The 2000kVA, 415V, % Z = 5.75% (ETAP, 2018), secondary full load ampere is 2,782.5A.

This shows that if there was a 3-Phase Bolted fault on the secondary of the transformer then the maximum fault current that could flow through the transformer would be the ratio of $\frac{100}{5.75}$ times the FLC of the transformer, i.e. 17.39 x the FLC = 48,386A.

Based on the infinite source method at the primary of the transformer; a quick calculation for the Maximum Fault Current at the transformer secondary terminals is $AFC = \frac{FLC}{\%_{PU}Z}$ $i.e$ $AFC = \frac{2,782.5}{0.0575} = 48,390A$. This is further illustrated with Table 1.

Table 1. Full Load Current (FLC) Calculation for 2-winding transformer characteristics

	MVA_T	Z%	Transf. Primary		Transf. Secondary	
			FLC1	AFC1	FLC_2	AFC2
Scenario 1	1	2.5	52.5	1,810	1391.2	55,648
Scenario 2	1	4	52.5	1,193	1391.2	34,780
Scenario 3	2	5.75	105.0	1,603	2782.4	48,390
Scenario 4	2	7.5	105.0	1,265	2782.4	37,099
Scenario 5	3	5	157.5	2,540	4173.6	83,472
Scenario 6	3	7.5	157.5	1,810	4173.6	55,648
Scenario 7	5	7.5	262.4	2,762	6956.0	92,747
Scenario 8	5	10	262.4	2,187	6956.0	69,560
Scenario 9	7.5	10	393.6	3,028	10434.0	104,340
Scenario 10	7.5	12.5	393.6	2,540	10434.0	83,472

For instance, for quick calculation; it is helpful to determine the fault current on the secondary of a transformer for the purpose of selecting the appropriate switchgear parameters. This is done in anticipation of providing an overcurrent protective device that can adequately interrupt the expected fault current values. However, the main breaker that is to be installed in the circuit on the secondary of the transformer is expected to have a kA Interrupting Rating greater than 49,000A. Meanwhile, if the actual relevant parameters of the connected motors are not known, then assume the contribution to be 4 x FLC of the transformer. Therefore, in this case, the feeders would be sized in such a way as to be able to withstand the full load current of the magnitude:

48,386 + (4 x 2,782.4) = 59,516A.

2.1.2 Generator Fault Current

Considering equation 6; in certain aspects, the generator fault current differs from that of the transformer, as shown in the calculations displayed below. For instance, appraising a 2000kVA generator whose rated capacity is given as: 1600kW, 0.8% PF, 415V. Recall that as stated in equation (7), the system full Load current (FLC) is obtained as follows:

$$FLC = \frac{kVA}{\sqrt{3}\, x\, V_{L-L}}$$

$$FLC = \frac{200}{1.732\ x\ 0.415} = 2{,}782.5A$$

Sub-transient X" values for this size of generator is 0.19 (ETAP, 2018). The Available Fault Current (AFC) is estimated as:

$$AFC = \frac{FLC}{X"} = \frac{2{,}782.5}{0.19} \quad i.e.\ AFC = 14{,}642A$$

So, the fault current of a 2000kVA Generator is a lot less than a 2000kVA transformer. The reason is that the transformer impedance value and the generator reactance value are different. In other words, it is in the following range: %Z of Transformer 5.75 as against that of %Z of Generator which is 19.

2.1.3 Utility MVA at the Primary of the Transformer

Step 3: From equation (7) above, just as the secondary side parameters have been obtained; thus, to determine the transformer primary full load current.

$$FLC\ (primary) = \frac{power}{Voltage\ x\sqrt{3}} \qquad (9)$$

Step 4: As depicted in equation (9); calculate the available fault current (AFC) primary by developing equation (8) based on high voltage (HV) side's FLC, i.e. at 11kV.

$$AFC(primary) = \frac{11kV}{\sqrt{3}} x \frac{1}{\frac{11^2}{MVA_{Utility}} + (\frac{11^2}{MVA_{Transformer}} x \frac{Z_{Transformer}}{100})} A \quad (10)$$

For this purpose, the MVA data for transformer, which are 2000kVA, 11/0.415kV, Z = 5.75%; can be deployed in equation (9)

MVA Value: The high voltage (HV) fault level (MVA_{sc}) taken as 250MVA for a 11kV system. Note that: $\frac{2000kVA}{2000} = 1\ MVA$

Hence, the MVA value is:

$$\text{MVA} = \frac{1\text{MVA}}{\text{Z}_{\text{pu}}} = \frac{1\text{MVA}}{0.0575} = 17.39\text{MVA}$$

Using the admittance method to calculate fault current; equation (11) is developed as:

$$\frac{1}{\text{MVA}_{Utility}} + \frac{1}{MVA_{Transformer}} = \frac{1}{\text{MVA}_{\text{SC}}} \quad (11)$$

So, from equation (11); the following calculation is obtained:

$$\frac{1}{250} + \frac{1}{17.39} = \frac{1}{MVA_{SC}}$$

$$0.004 + 0.06 = \frac{1}{MVA_{SC}}$$

i.e.

$$MVA_{sc} = \frac{1}{(0.004 + 0.06)} i.e. MVA_{sc} = 15.625\text{MVA}$$

Thus, from equation (8) above, for AFC

$$AFC\ at\ 415V = \frac{MVA_{SC}}{(1.732\ x\ 0.415)}$$

$$AFC\ = \frac{15.625}{0.7188} = 21.738\ kA$$

i.e. AFC = 21, 738A

From the foregoing; the illustrative diagram of the results of the above calculations using manual steps is as presented in Figure 3.

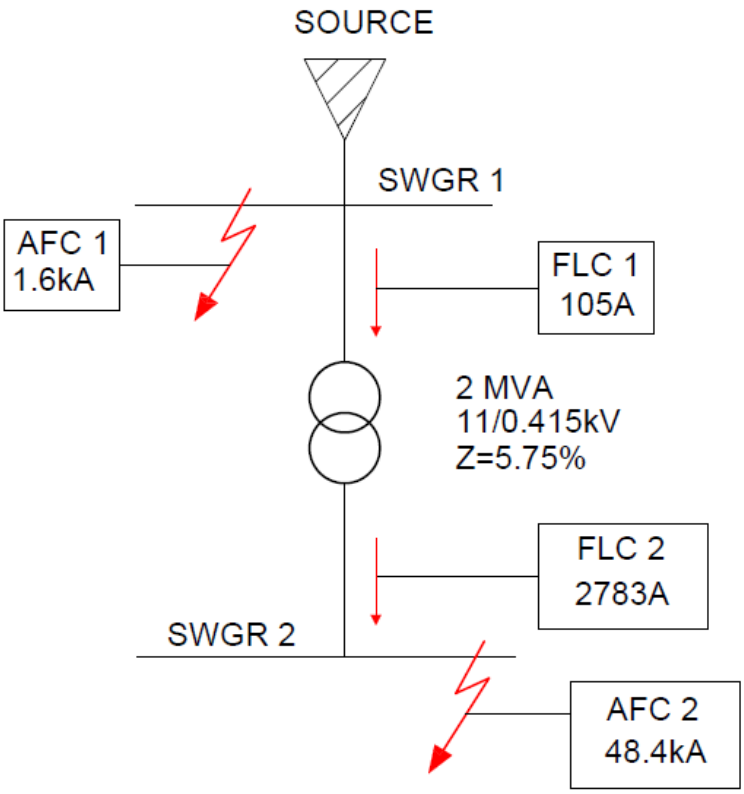


Figure 3. Example of Hand Calculation Result

For very large and complex network, this hand calculation is very tedious. To overcome this, computer software is used. In this work, ETAP software is deployed (ETAP, 2018).
The 415V Fault Current value at the secondary of the 2000kVA transformer based on an infinite Utility Source at the Primary of the transformer is calculated as 48,390A, while the 415V Fault Current value at the secondary of the 2000kVA transformer based on a 250MVA Utility Source at the Primary of the transformer is calculated as 21,738A. When cable and its length is added to the circuit, the fault current in a 415V system will decrease to a smaller value (Davidson, 2005). To add cable design details into the calculation, then equation (12) is deployed as:

$$Cable\ MVA\ Value,\ MVA_{SC} = \frac{kV^2}{Z_{cable}} \qquad (12)$$

Obtain values the of cable's reactance, X, and resistance, R, for the purpose of calculating the value of cable impedance, Z, as shown in equation 12 (PSEC-IEEE, 2000).

Note that it is crucial to assess the fault current value in a system to select and install the appropriate size of the overcurrent protective device (OCPD). Thus, the reduction in the fault current value at the primary side of the transformer results in the reduction of the AFC as shown in calculations (Preethi & Manik, 2016). It is of necessity to add the term (4 x FLC) as the motor contributions if the infinite method is applied to the calculation of fault current. This will ensure that the calculated fault current value will be very conservative. In other words, the real calculated value will never be reached thereby leading to the reduction in failures of any potential overcurrent protection device resulting from the fault current (PSEC-IEEE, 2000).

2.2 Power System Typical Network Arrangement

The sources connected to the chosen model network comprise of two units of gas turbine generator sets tagged GTG-01 and GTG-02 and a standby gas turbine-generator set named GTG-03; each of these is rated at 2.5 MW. The 2-black start/emergency diesel generator sets labelled as EDG-04 and EDG-05 each rated at 750kVA come up when the main gas turbine generators fail, this is always set to be running in slightly non-typical operating mode but never in normal operating mode. Other power equipment in consideration includes 3 units of Power transformer each rated 2 x 2MVA, 11/0.415kV and 1 x 3MVA, 11/4.16kV, medium voltage (MV) lumped asynchronous motor loads M1 and M2, and Low voltage (LV) lumped loads including induction motor loads M3-M8.

The parameters for the equipment are derived from manufacturers' data when provided (generators, motors, and power transformer ratings). Typical (standard) parameters from ETAP Library are used when data are not provided. This can be seen in Table 2-5 (ETAP, 2018).

2.2.1 Algorithm of power system simulation

In order to achieve the criteria for the best selection of the switchgear; Figure 4 is providing a guide using the flow chart of the procedure for the ETAP simulation.

2.2.2 Power System Network Modelling

The one-line diagram of the power system network shown in Figure 5 is modelled as an impedance diagram from which impedance values and data for simulation are derived. Fig. 6 shows the impedance diagram of the power system network with 14 buses, 13 branches and 38 loads. The input data shown in Tables 2, 3, 4 and 5 are derived from Figure 6, including generator (synchronous machine) data, transformer data, feeder data and bus data. The values attributed to the impedances are expressed in per unit of the common base power which is taken as S_b = 100 MVA.

Table 2. Generation input Data

Gen Name	Bus Name	Rating/Limit	Rated kV	MW	MVAr	Amperes	% PF	% Generation
GTG-01	SWGR-01	2.5 MW	11	1.498	0.841	90.19	87.2	59.9
GTG-02	SWGR-01	2.5 MW	11	1.498	0.841	90.19	87.2	59.9
GTG-03	SWGR-01	2.5 MW	11	1.498	0.841	90.19	87.2	0 (standby)

Table 3. Transformer Input Data

Transf. Name	Primary Bus			Secondary Bus			Full Load kVA	Nom. kVA	% Imped. (%Z)	X/R	% Loading
	Name	Config.	Volts (L-L)	Name	Config.	Volts (L-L)					
TR-01	SWGR-01	Delta	11000	SWGR-03A	Star	415	2.000	2.000	6.25	6	48.2
TR-02	SWGR-01	Delta	11000	SWGR-03B	Star	415	2.000	2.000	6.25	6	29.5
TR-03	SWGR-01	Delta	11000	SWGR-02	Star	4160	3.000	3.000	5.50	10.67	64.7

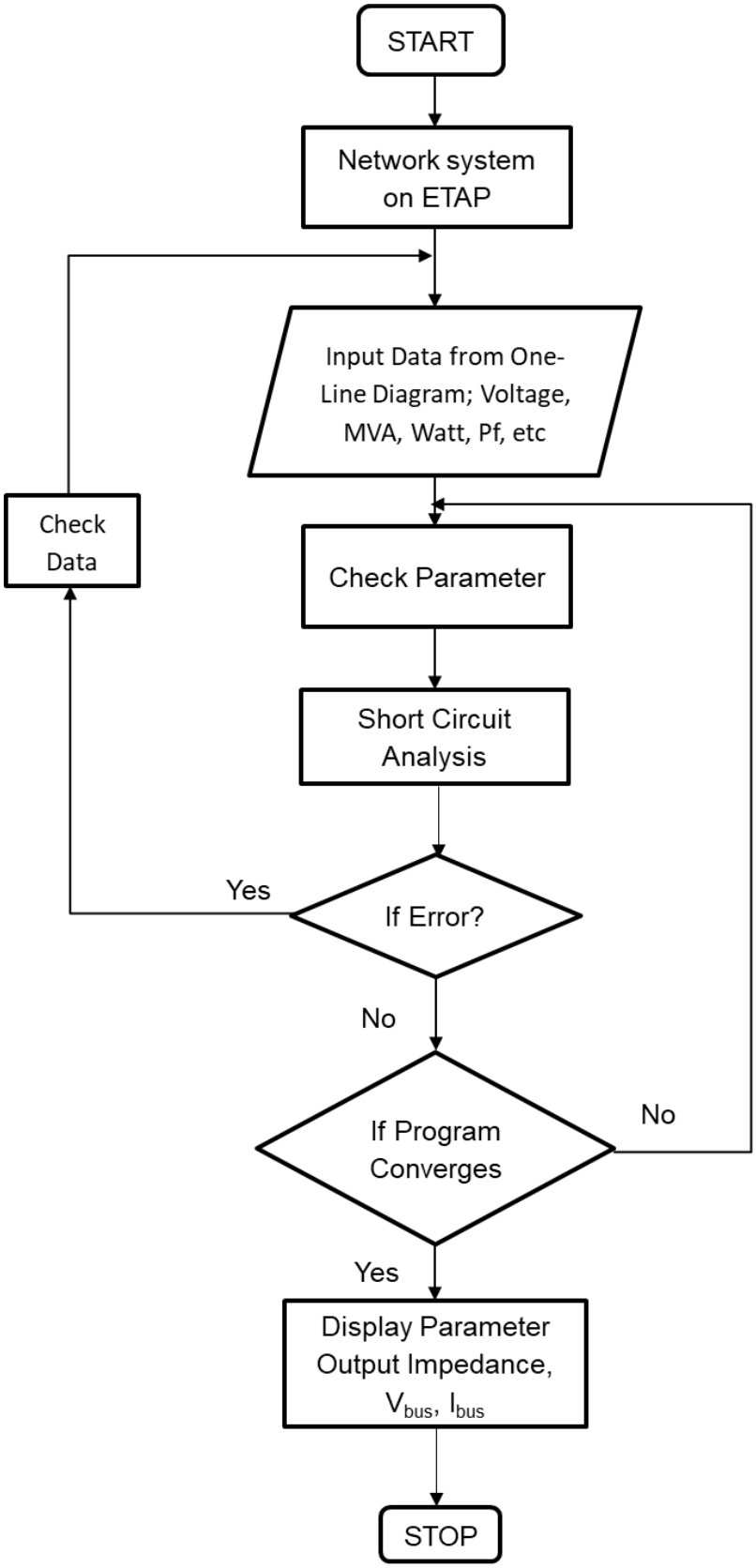


Figure 4. Flow chart for ETAP simulation steps for the best selection criteria

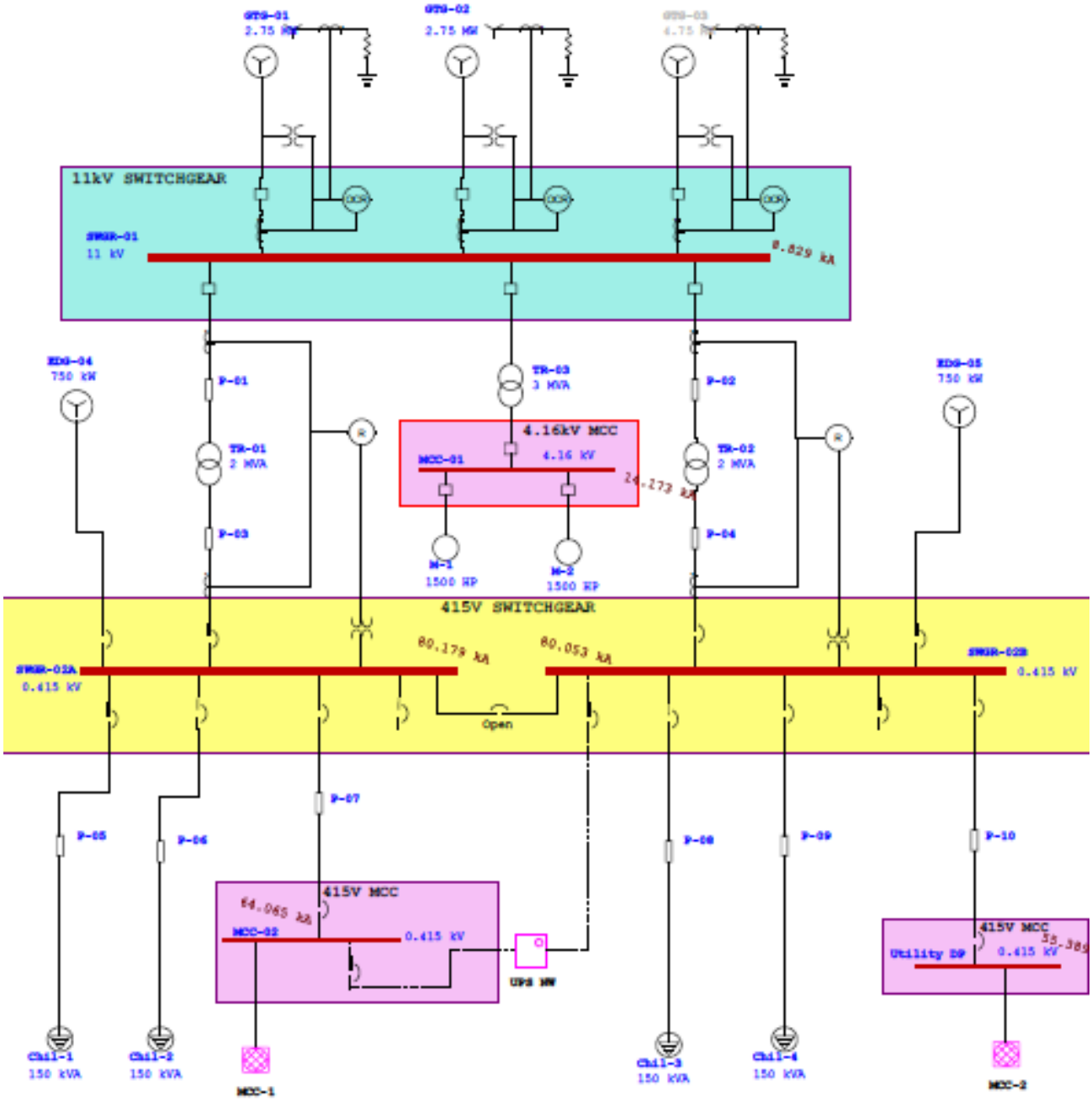


Figure 5. Simplified one-line diagram (network model) of the electrical power system.

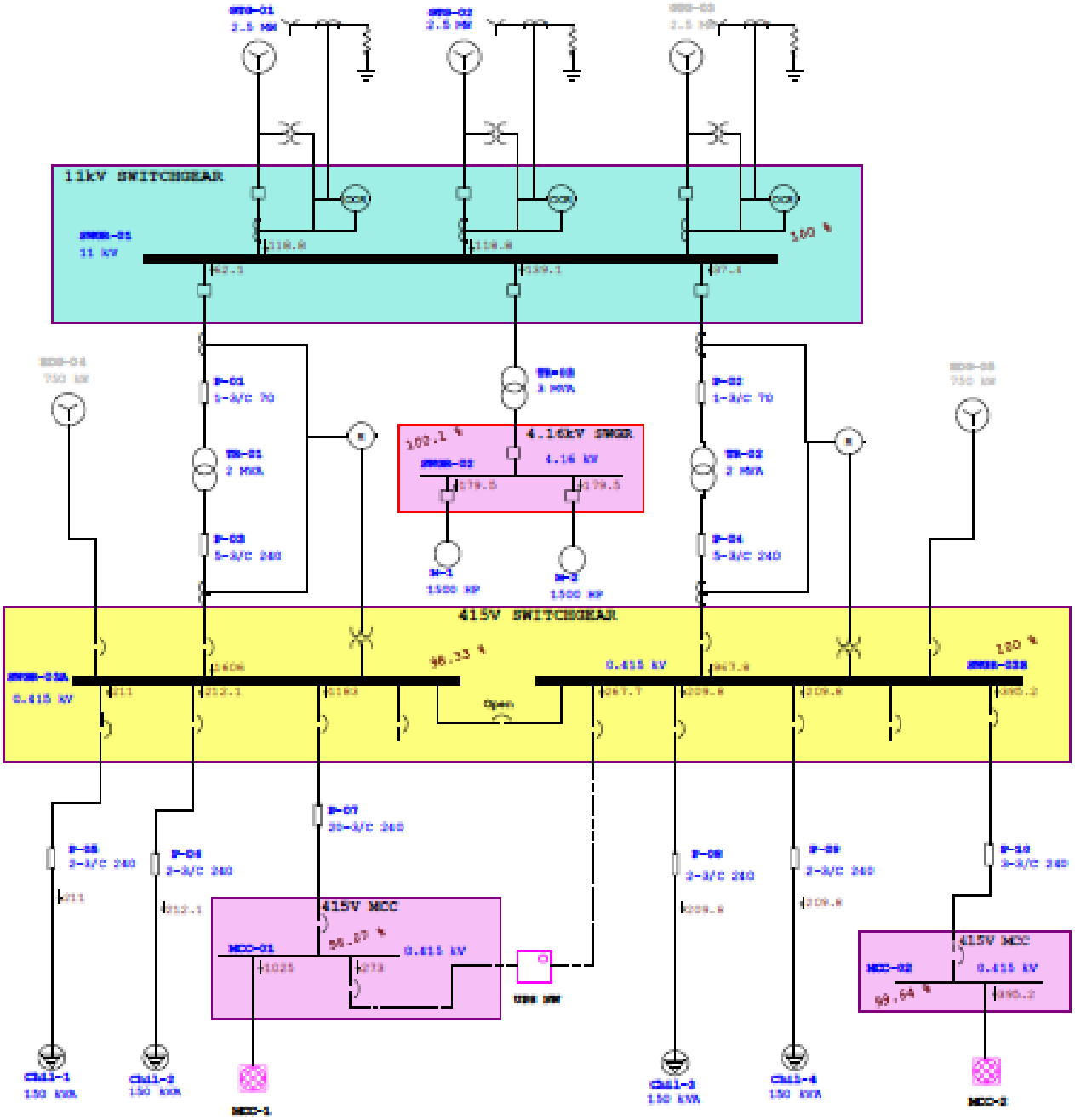


Figure 6. Impedance diagram of the power system network with 14 buses

Table 4. Bus Input Data

Bus Name	Nominal kV	Amp Rating	Voltage	MW Loading	Amp Loading	% Loading
SWGR-01	11	2000	100	3.933	237.6	11.9
SWGR-02	4.16	1200	100.08	2.391	358.9	29.9
SWGR-03A	0.415	4200	98.33	0.927	1607	38.3
SWGR-03B	0.415	4200	100.03	0.576	967.8	23
MCC-01	0.415	4200	98.07	0.685	1183	28.2
MCC-02	0.415	1200	99.64	0.245	395.2	32.9

Table 5. Feeder Input Data

Feeder Name	From Bus	To Bus	Rating 1	Rating 2	Allowable	Amp Flow	% Loading	% Voltage Drop
P-01	SWGR-01	Bus1	200 ft	1x3/C 70	197 A	62.14	24.4	0.02
P-02	SWGR-01	Bus2	200 ft	1x3/C 70	197 A	37.42	14.9	0.01
P-03	Bus3	SWGR-03A	300 ft	5x3/C 240	1842 A	1607	67.6	1.12
P-04	Bus4	SWGR-03B	300 ft	5x3/C 240	1842 A	967.8	41.3	0.68
P-05	SWGR-03A	Bus5	600 ft	1x3/C 240	357.7 A	212.1	44.2	1.44
P-06	SWGR-03A	Bus6	600 ft	1x3/C 240	168 A	212.1	94.9	2.81
P-07	SWGR-03A	SWGR-01	300 ft	15x3/C 240	7370 A	1183	12.6	0.21
P-08	SWGR-03B	Bus7	600 ft	1x3/C 240	357.7 A	209.8	44	1.43
P-09	SWGR-03B	Bus8	600 ft	1x3/C 240	357.7 A	209.8	44	1.43
P-10	SWGR-03B	MCC-02	200 ft	3x3/C 240	1105 A	395.2	26.6	0.29

3.0 RESULTS AND DISCUSSION

The simulated results are presented in the following sub-sections.

3.1 System Simulation

The following series of arrangement of the power equipment for generation and distribution systems are used for the simulation (see Figure 5). Whereby the main generators (GTG-01 and GTG-02), the standby main generator (GTG-03) and emergency (i.e. black-start) generators (EDG-04 and EDG-05) are connected to the distribution system. The 415V bus-tie between bus A (Swgr-03A) and bus B (Swgr-03B) is open. Whilst the lumped electrical loads relate to the closure of all other distribution interconnections. It is also important to note that fault currents are calculated for 100 milliseconds after the inception of fault.

So, the three operating voltage levels namely, 415V, 4160V and 11000V are deployed for the simulation of the network in order to determine the optimum value of the system generating voltage based on the various short circuit current levels. Thus, consideration of switchgear requirements and rating availability in conjunction with the calculated fault currents dictate suitability of the switchgear. In other words, regarding the voltage level of 415V; the switchgear would naturally require higher rated current values to handle the same magnitude of power quantity than those switchgear operating at 4160V and 11000V voltage level.

The parameters for the systems under investigation are shown in Table 6. Whereby a total of three (i.e., 1, 2 and 3) scenarios is simulated. The cases are as presented in which the current flow for short circuit operating conditions of the six busbars (i.e., SWGR-01, SWGR-02, SWGR-03A, SWGR-03B, MCC-01 & MCC-02) are considered.

Table 6. Operation scenarios of the system with the application of 3-phase fault

Study Case	Main Generator	Operation Scenario	3 Phase Fault Applied to
1	GTG-01 & GTG-02	Tie-Bus open with TR-01 & TR-02 CBs closed	SWGR-01 SWGR-02
2	GTG-01 & GTG-02	Tie-Bus closed with TR-01 CB closed & TR-02 CB open	SWGR-03A SWGR-03B
3	GTG-01 & GTG-02	Tie-Bus closed with TR-01 CB & TR-02 CB closed (both transformers running in parallel)	MCC-01 MCC-02

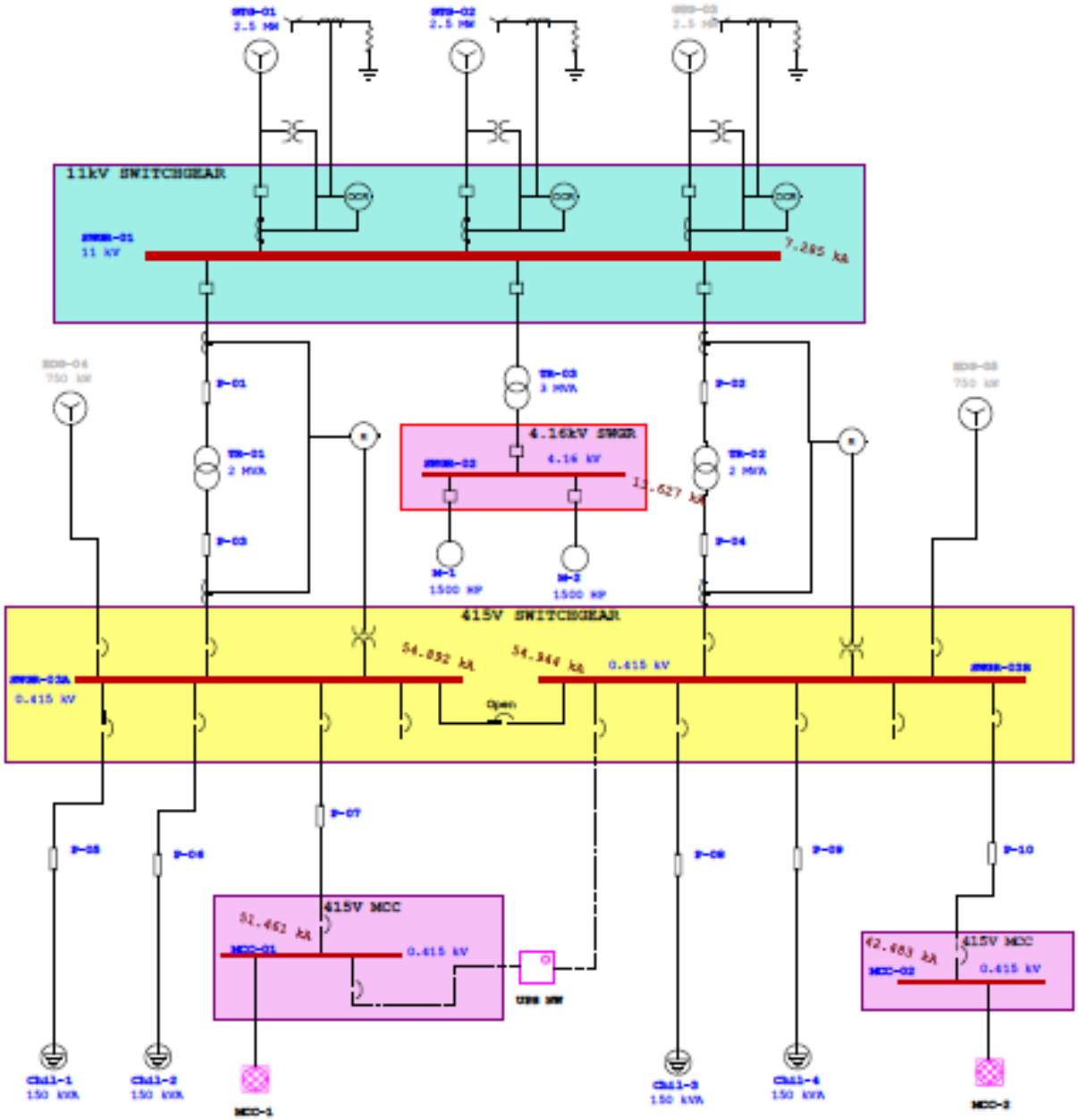


Figure 7. Layout of the distribution of fault current along the network branches for study case 1

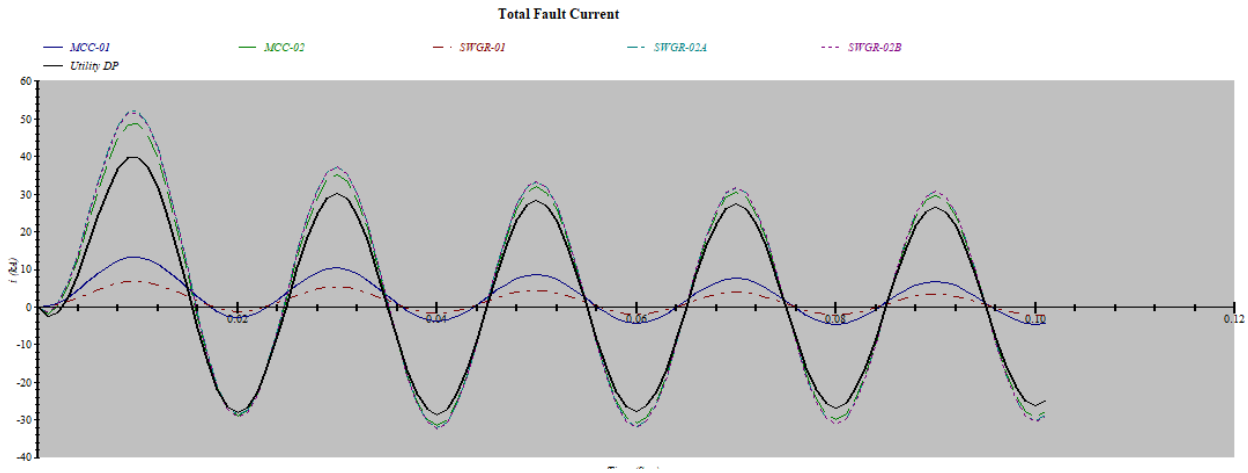


Figure 8. Graph of total fault current against time

Table 7. Operation of Short Circuit Currents at Diverse Fault Levels on Different Categories of Switchgear

Study Case	Fault at	Nominal kV	I''_k (kA)	I_p (kA)	I_k (kA)	I_b (kA)	I_{dc} (kA)	X/R ratio L-G
1	SWGR-01	11	2.93	7.29	0.63	2.22	1.38	8.5
	SWGR-02	4.16	5.62	13.63	2.99	4.38	1.78	8.0
	SWGR-03A	0.415	27.22	54.89	20.22	26.64	15.35	3.2
	SWGR-03B	0.415	27.40	54.94	20.22	26.63	15.16	3.0
	MCC-01	0.415	26.19	51.46	19.56	25.63	13.33	2.9
	MCC-02	0.415	23.34	42.48	17.52	22.55	8.41	2.2
2	SWGR-01	11	2.90	7.21	0.63	2.21	1.38	8.8
	SWGR-02	4.16	5.59	13.56	2.99	4.37	1.78	8.1
	SWGR-03A	0.415	30.98	61.23	20.22	29.63	16.84	3.0
	SWGR-03B	0.415	30.98	61.23	20.22	29.63	16.84	3.0
	MCC-01	0.415	29.60	56.90	19.56	28.39	14.33	2.7
	MCC-02	0.415	25.73	45.93	17.52	24.64	8.65	2.1
3	SWGR-01	11	2.93	7.26	0.63	2.22	1.38	8.5
	SWGR-02	4.16	5.62	13.61	2.99	4.38	1.78	8.0
	SWGR-03A	0.415	41.79	87.19	28.24	40.10	27.55	3.6
	SWGR-03B	0.415	41.79	87.19	28.24	40.10	27.55	3.6
	MCC-01	0.415	39.30	78.36	27.02	37.88	21.96	3.1
	MCC-02	0.415	32.53	58.35	23.33	31.43	11.21	2.1

Table 8. Influence of Operation of 3-Phase Peak Short Circuit Current on Various Switchgear Classes

STUDY CASE	BUS NAME	NOMINAL KV	OEM-KA RATING (AIC)	3-PHASE KA DUTY	REMARK
1	SWGR-01	11	50	7.26	OK
	SWGR-02	4.16	50	13.61	OK
	SWGR-03A	0.415	65	54.49	OK
	SWGR-03B	0.415	65	54.54	OK
	MCC-01	0.415	65	51.11	OK
	MCC-02	0.415	65	42.25	OK
2	SWGR-01	11	50	7.21	OK
	SWGR-02	4.16	50	13.56	OK
	SWGR-03A	0.415	65	61.23	OK
	SWGR-03B	0.415	65	61.23	OK
	MCC-01	0.415	65	56.90	OK
	MCC-02	0.415	65	45.93	OK
3	SWGR-01	11	50	7.26	OK
	SWGR-02	4.16	50	13.61	OK
	SWGR-03A	0.415	65	87.19	Not Acceptable
	SWGR-03B	0.415	65	87.19	Not Acceptable
	MCC-01	0.415	65	78.36	Not Acceptable
	MCC-02	0.415	65	58.35	OK

3.2 Discussion of Results

As stated earlier, the collection of simulations was performed using Electrical Transient Analyzer Program (ETAP) Version V16.2. (ETAP, 2018). Wherein the three-phase fault current magnitudes calculated by the software are summarized in Table 7. The results of case-1 established that the three-phase symmetrical fault current, I''_k. In this case, the influence of the generation of short circuit phenomenon on busbars SWGR-03A and SWGR-03B (i.e. the two bus bars to which the two emergency diesel generators are connected) are 54.89kA and 54.94kA respectively. These values are well within the fault rating of 65 kA for which low voltage switchgears are readily available. The other two cases were as presented

in the Table 7. However, Table 8 presents the peak short circuit current, $I_{p,}$ with the rated values of tested and available switchgear equipment in the market. In line with this, Figure 7 presents the fault distribution on the electrical network for the study cases while Figure 8 provides information on the switchgear's capacity to withstand the total fault current as depicted in the graph presented therein (i.e. Figure 8).

From the foregoing, Table 6 provided critical data on the system's analytical parameters while Tables 7 and 8 address the catastrophic effect of high current flow in electric equipment in power distribution network. Needless to state that the resulting effect is arcing effect which is a direct response of untamed thermal excursion with unequalled overheating of the electric equipment alongside its attendant production of excessive force and arc, which react with air to eventually produce a series of explosions of great magnitude.

3.3 Selection Criteria

From the above results, it is clear that the short circuit analysis is capable of determining the magnitude of current flow in the power system equipment operating under fault conditions. However, if the short circuit capacity of the system exceeds the capacity of the protective device, then a dangerous situation is thus recorded in terms of explosion. Hence the best selection procedure is to assess the magnitude of the short circuit fault potentials of the electric equipment. This would then provide the platform for appropriate selection of appropriately matching switchgear equipment. However, this must possess electrical current capacity that would be greater than the system short circuit capacity.

4.0 CONCLUSION AND RECOMMENDATION

From the simulated results, the computation of magnitude of fault current distribution at various points in the network was investigated. These fault current values were compared with the ratings of standard original equipment manufacturer (OEM) switchgears to confirm that the selected switchgears have sufficient capacity to withstand the expected magnitude of the short circuit energy at each point in the process of the power system operation. Meanwhile, it is noteworthy that the magnitude of the fault currents that exceed equipment ratings can result into an extensive damage to the operation of the power system. This also poses serious threats to human life and property. Note that no substation equipment, motor control centres, switchboards and switchgear can be purchased without sound knowledge of the complete short circuit values for the entire power system. Thus, the system short circuit values must be calculated with precision whilst all electrical equipment connected to the network must be able to withstand, without failure or damage, the maximum short circuit conditions of certain dimensions. This research presents these results to overcome the occurrence of needless injury and avoidable fatality to workers by reducing undesired effects of faults on the power systems to the barest minimum. However, failure to achieve this goal would result in a catastrophic effect that could lead to the earlier expressed challenges (i.e., injury and fatality).

Moreover, it was observed that short circuit (fault) level is an important parameter in the selection of switchgears. It is thus important that the short circuit calculations are consistently processed and periodically updated to ensure healthy operating status for the protection of power equipment as well as the lives of workers. It must be stated herein that this calculation is in fact far less expensive than diverse costs associated with electrical system failure with its resultant accidents. So, to maintain the power system integrity and

reliability, it is important to perform an arc flash study to establish the risk levels, for proper reconfiguration of the system layout to avoid hazards. So also, of importance is the use of arc resistant equipment to reduce the attendant hazards as well as the conduct periodic power system integrity checks for those equipment whose useful life counts are between 10 years and 20 years of installation. Lastly, the power system integrity checks are essentially important to ensure that the switchgear is operating within the appropriate values of the arc interruptible current (AIC) rating as well as the short circuit current rating (SCCR).

REFERENCES

Al-Mohammed A. H. & Abido M.A. (2014), A Fully Adaptive PMU-Based Fault Location Algorithm for Series-Compensated Lines, in *IEEE Transactions on Power Systems*, 29(5), 2129-2137, doi:10.1109/TPWRS.2014.2303207.

Chen, M., Zhai, J., Lang, Z. Q., Sun, F., & Hu, G. (2012). "A Nonlinear Frequency Analysis-Based Approach for Power Cable Insulation Fault Detection". *COMPEL - The International Journal for Computation and Mathematics in Electrical and Electronic Engineering*, 31(2), 369–386. doi:10.1108/03321641211200482.

Davidson I. E. (2005) "Utility Asset Management in the Electrical Power Distribution Sector", IEEE/PES 2005 Power Engineering Society Inaugural Conference and Exposition in Africa, 11-15 July 2005, pp. 338-343.

ETAP (2018): Electrical Transient Analyzer Program, Version V16.2, https://etap.com/

Preethi M. and Manik H. (2016), Fast and Accurate Fault Detection in Transmission Line using Wavelet Transform, *IJIRST- International Journal for Innovative Research in Science & Technology*, 2, 11/092, 523-531

PSEC-IEEE, (2000), Power Systems Engineering Committee of the IEEE Industry Application Society: "IEEE Recommended Practice for calculating ac short circuit currents in industrial and commercial power systems- (IEEE Violet Book) P551, D1, 12 pages, https://web.fe.up.pt/~ee03186/normas%20do%20IEEE%20para%20calculo%20de%20cc.pdf (Accessed on Monday June 10, 2019).

Rambabu M., Venkatesh, M., SivaKumar, J.S.V. and AyyaRao, T. S. L. V., (2015), Three Zone Protection by using Distance Relays in SIMULINK/MATLAB. *International Research Journal of Engineering and Technology (IRJET)*, 2(5), 810-819, www.irjet.net

Sarwar M., Mehmood F., Abid, M., Khan A. Q., Gul S. T. and Khan A. S. (2019), High Impedance Fault Detection and Isolation in Power Distribution Networks using Support Vector Machines, *Journal of King Saud University - Engineering Sciences*, https://doi.org/10.1016/j.jksues.2019.07.001

Wu F., Yin S. and Karimi H. R. (2014), "Fault Detection and Diagnosis in Process Data using Support Vector Machines", *Journal of Applied Mathematics*, 2014, 1-9. http://dx.doi.org/10.1155/2014/732104 .

Yu, L. Y., Minceff, I., Hamilton, D. W., & Bottrell, G. W. (1982). Motor Contribution during Three-Phase Short Circuit Fault. *IEEE Transactions on Industry Applications*, IA-18(6), 593-599.